Pis'ma v ZhETF, vol. 103, iss. 2, pp. 113 – 118 © 2016 January 25

Peierls distortion and electron bands in phosphorus allotropes

L. A. Falkovsky[1)]

Landau Institute for Theoretical Physics of the RAS, 142432 Chernogolovka, Russia

Vereshchagin Institute of the High Pressure Physics of the RAS, 142190 Troitsk, Russia

Submitted 18 November 2015

A small difference between the rhombohedral phosphorus lattice (A-7 phase) and the simple cubic phase as well as between phosphorene and the cubic structure is used in order to construct their quasiparticle band dispersion. We exploit the Peierls idea of the Brillouin zone doubling/folding, which has been previously employed in consideration of semimetals of the V period and IV–VI semiconductors. In a common framework, individual properties of phosphorus allotropes are revealed.

DOI: 10.7868/S0370274X16020065

I. Introduction. In the last decade, much progress in study of the graphene monolayer has been achieved [1]. Graphene turned out to be a material with remarkable properties: the universal optical conductivity $e^2/4\hbar$, light transmittance giving the fine-structure constant, the Coulomb renormalization of the Fermi velocity. However, absence of a band gap does not permit to use graphene in field-effect transistor devices. This is the reason to seek other two dimensional materials with sizable gap and high mobilities. One of such promised substances becomes phosphorene, i.e., a monolayer of black phosphorus.

Element phosphorus belongs to the same period of the periodic table as semimetals As, Sb, and Bi and contains two s and three p valent electrons. There exist at least three phosphorus allotropes: simple cubic (sc), rhombohedral (bismuth A-7 symmetry), and orthorhombic (A-17). Orthorhombic black phosphorus (BP) is the most stable allotrope at ambient pressure and temperature. At 4.5 GPa, the structure changes from A-17 to A-7, which transforms to the sc one at 10 GPa. There are also two phase transformations at 137 and 262 GPa. The sc allotrope possesses one remarkable property – it becomes a superconductor with maximum $T_c = 9.5$ K under pressure 32 GPa [2, 3], and such high temperature of the superconducting transition was explained in the Ref. [4] by the electron-phonon coupling. An anisotropic optical response [5] with a high mobility of carriers promises BP as viable linear polarizers for applications. The high mobility, tunable bandgap, and linear dichroism along two in-plane directions make few-layer phosphorus a candidate for future electronics and optoelectronics.

Recently, the success was achieved in fabricating field-effect transistors [6–9] based on few-layer BP. Comparing to graphene, BP has an advantage possessing a quasiparticle band gap. The band gap value of monolayer (0.75–2.5 eV in various calculations) tends to smaller values (0.1–0.36 eV) in bulk BP [10–12]. The calculations within the tight-binding approach [13, 14] or modern first-principal ones [12, 15, 16] give the different values of the band gap. For bulk BP, that is the direct gap at the Z point [14] of the order of 0.3 eV or the indirect band [17] between the valence-band maximum at the Z point and the conduction-band minimum at Γ. Sometimes, the variations in the band gap value are explained by the many-particle correlation effects [15]. According to Ref. [18], the self-energy correction enlarges the band gap from 0.8 to 2 eV, however, the optical absorption peak is reduced to 1.2 eV, that can be broadly tuned by changing the number of stacked layers. The effective masses display anisotropy in BP. In the one direction, both for electrons and holes, the effective mass is of the order of the free-electron mass, however the masses are five times lighter in other two directions. The authors of Ref. [19] assume that the valence and conduction bands have a different parity and interact strongly to one another.

The first-principal calculations do not lead to analytic results giving the inconsistent values for a band gap and effective masses in BP. Therefore, such calculations are usually added by the qualitative considerations. By that reason, it is reasonable to use the Peiers idea of the unit-cell doubling. As known, the crystal structures of the V group semimetals As, Sb, and Bi can be obtained from the sc lattice by small displacements of atoms. The corresponding deformation called as a Peierls distortion was employed for the evaluation

[1)]e-mail: falk@itp.ac.ru

of the electron dispersion in Bi and Sb as well as in IV–VI compounds [20–23]. In this work, we take the Peierls idea as a background in constructing an effective low-energy Hamiltonian for phosphorus allotropes. Within a common framework, electron band-dispersions are evaluated in an explicit form for the sc, A-7 allotropes, and phosphorene.

II. Band dispersion for a semimetal with the rhombohedral lattice and two atoms in the unit cell. Here we consider the electron dispersion of the sc and A-7 lattices for the elements of the V group, using the Peierls idea of the unit-cell doubling. There are one atom in the unit cell of the sc lattice and two atoms in the A-7 unit cell. The correct Bloch functions of the zeroth approximation are constructed from the Wannier orbitals $p_i(\mathbf{r})$ as a sum over the lattice sites n and two atoms A in the unit cell as

$$\psi_i(\mathbf{r}) = \sum_{n,A} e^{i\mathbf{k}\mathbf{r}_n^A} p_i(\mathbf{r} - \mathbf{r}_n^A), \tag{1}$$

where $i = x, y, z$ numerates the p_i orbitals. We assume that the s orbitals are located more deeply and are separated well from the p_i bands.

In the sc lattice, an atom with the coordinates (000) has six nearest neighbors at the distance a in $\pm(100)$, $\pm(010)$, and $\pm(001)$ sites and twelve next-nearest neighbors in the sites like (110). The electron–lattice interaction H_0 of the cubic symmetry gives the following matrix elements between the first neighbors

$$\xi_{xx} = \xi_0 \cos k_x a + \xi_1(\cos k_y a + \cos k_z a) \tag{2}$$

and between the next-nearest neighbors

$$\eta_{xy} = \eta_0 \sin k_x a \sin k_y a,$$
$$\eta_{xx} = \eta_1 \cos k_y a \cos k_z a + \eta_2 \cos k_x a(\cos k_y a + \cos k_z a). \tag{3}$$

Here the hopping integrals are

$$\begin{aligned} \xi_0 &= 2\langle p_x(000)|H_0|p_x(100)\rangle, \\ \xi_1 &= 2\langle p_x(000)|H_0|p_x(010)\rangle, \\ \eta_0 &= -4\langle p_x(000)|H_0|p_y(011)\rangle, \\ \eta_1 &= 4\langle p_x(000)|H_0|p_x(011)\rangle, \\ \eta_2 &= 4\langle p_x(000)|H_0|p_x(110)\rangle, \end{aligned} \tag{4}$$

and the arguments of the p_i orbitals indicate the sites where these orbitals are centered. The remaining matrix elements are given by cyclic permutation of the indices. In Fig. 1, the electron dispersion is shown for the sc lattice with $\xi_0 = 4$ eV, $\xi_1 = -1$ eV, $\eta_0 = -0.2$ eV, $\eta_1 = \eta_2 = 0.2$ eV. If the interatomic distance a is short enough and the nearest hopping integrals ξ_0 and ξ_1 have a typical atomic values, such the crystal should be a good metal. Then three valent electrons can occupied only half places in these three bands degenerate to spin. It is not surprising that phosphorus becomes a superconductor under pressure, when it displays the sc structure.

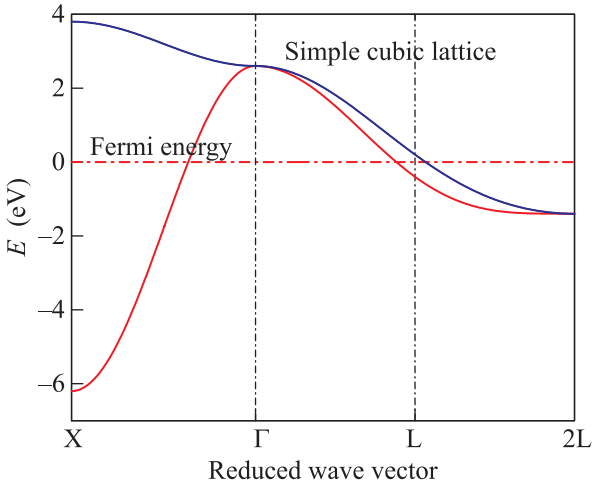

Fig. 1. (Color online) Three electron bands for a metal with a simple cubic lattice; the two-fold degenerate band is shown in a thick line

At high pressure from 40 to 80 kbar, phosphorus has the rhombohedral structure (A-7 phase). This structure can be formed from the sc phase by a small relative displacement of two face-centered sublattices. Thus, in the unit cell, we get two atoms shown in Fig. 2 by the cross and empty circles and obtained from the atoms at the (000) and (111) sites in the cubic phase. In the A-7 phase, their rhombohedric coordinates become $\pm(0.25-u, 0.25-u, 0.25-u)$ with u equal to several percents. For bismuth and rhombohedral phosphorus, such

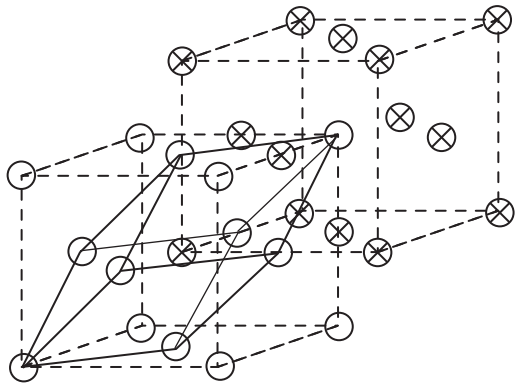

Fig. 2. Structure of the sc and A-7 lattices; two sublattices in A-7 are shown by crosses and empty circles, correspondingly

a distortion is of the order 5–10 %. For instance, in bismuth, the angles between bonds become 57° instead of 60° in the sc phase. The Peierls distortion results in the doubling of the unit cell volume. The primitive vectors for the face-centered lattice are

$$\mathbf{a}_i = a(011), \quad a(101), \quad a(110),$$

and the primitive vectors for the reciprocal lattice write

$$\mathbf{Q}_i = \pi(-1,1,1)/a, \quad \pi(1,-1,1)/a, \quad \pi(1,1,-1)/a.$$

The Peierls distortion can be represented as a result of the electron–lattice interactions of the rhombohedral symmetry D_{3d}, first, due to the sublattice shift

$$U(\mathbf{r}) = \mathbf{u} \cdot \nabla[V_A(\mathbf{r}) - V_B(\mathbf{r})] \equiv \mathbf{u} \cdot \mathbf{O} \tag{5}$$

in the (111) direction and, second, because of the deformation

$$E(\mathbf{r}) = \varepsilon_{ij} O_{ij}(\mathbf{r}) \tag{6}$$

affecting the angles between the bonds and described by the tensor ε_{ij}.

The Hamiltonian for the face-centered lattice with two atoms in the unit cell obtains the form

$$H(\mathbf{k}) = \begin{pmatrix} A & iU \\ -iU & A_Q \end{pmatrix}, \tag{7}$$

where A is the 3×3 matrix given by the matrix elements in Eqs. (2)–(4). The matrix A_Q is obtained from A by the substitution $\mathbf{k} \to \mathbf{k} + \mathbf{Q}_1 + \mathbf{Q}_2 + \mathbf{Q}_3$. The additional contributions to the matrices A and A_Q appears from the interaction $E(\mathbf{r})$, Eq. (6), and has the matrix elements

$$E_{xy} = e_0 + e_1(\cos k_x a + \cos k_y a) + e_2 \cos k_z a,$$

with the hopping integrals

$$\begin{aligned} e_0 &= \varepsilon_{xy}\langle p_x(000)|O_{xy}|p_y(000)\rangle, \\ e_1 &= \varepsilon_{xy}\langle p_x(000)|O_{xy}|p_y(100)\rangle, \\ e_2 &= \varepsilon_{xy}\langle p_x(000)|O_{xy}|p_y(001)\rangle. \end{aligned} \tag{8}$$

The 3×3 matrix U has the matrix elements of the doubling interaction, Eq. (5), as following

$$\begin{aligned} U_{xx} &= u_1 \sin k_x a + u_2(\sin k_y a + \sin k_z a), \\ U_{xy} &= u_3(\sin k_x a + \sin k_y a), \end{aligned} \tag{9}$$

where

$$\begin{aligned} u_1 &= 2\langle p_x(000)|O_x|p_x(100)\rangle, \\ u_2 &= 2\langle p_x(000)|O_y|p_y(010)\rangle, \\ u_3 &= 2\langle p_x(000)|O_y|p_y(100)\rangle. \end{aligned} \tag{10}$$

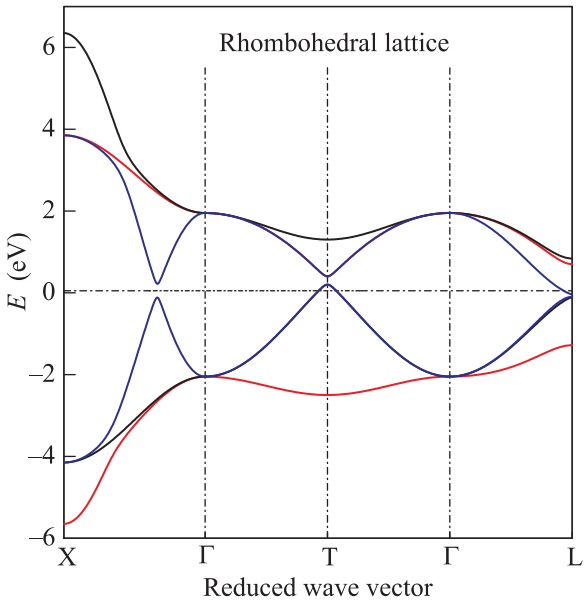

Fig. 3. (Color online) Band structure of a rhombohedral phosphorus with two atoms in unit cell; the holes/electrons are at the T/L points

Hamiltonian (7) gives six bands shown in Fig. 3. In this case, we get a semimetal with holes/electrons at the T/L points as it should be in bismuth. The following values of the hopping integral are taken (in eV): $\xi_0 = 4$, $\xi_1 = -1$, $u_1 = 0.25$, $u_2 = 0.15$, $u_3 = 0.5$, $\eta_0 = -0.3$, $\eta_1 = 0.15$, $\eta_2 = -0.1$, $e_0 = -0.1$, $e_1 = 0.12$, $e_2 = -0.4$. Another set of parameters can produce a semiconductor with the narrow band-gap. The largest hopping integrals ξ_0 and ξ_1 have the comparable values for semimetals of the V period and for the IV–VI semiconductors [21, 22]. The values of e_0, e_1, e_2, u_1, u_2, and u_3 parameters must be on the order of $0.1\xi_0$, because they are proportional to the Peierls weak distortion.

The spin-orbit interaction

$$\hat{\Delta} = -\frac{i}{3}\Delta_{so} \begin{pmatrix} 0 & \sigma_z & \sigma_y \\ -\sigma_z & 0 & \sigma_x \\ \sigma_y & -\sigma_x & 0 \end{pmatrix},$$

where σ_i are the Pauli matrices, should be added to the matrices A and A_Q for antimony and bismuth, where Δ_{so} is of the order of ξ_1. The band dispersion for the spin-splitting $\Delta_{so} = 1$ eV is shown in Fig. 4.

III. Band dispersion for phosphorene. The structure of BP consists of two puckered surfaces. One such the surface called phosphorene is shown in Fig. 5. Now we apply the idea of the Peierls doubling to phosphorene. In the A-7 case of doubling, we use the unit cell with two atoms. However, in the unit cell of phosphorene, there are four atoms each with three p_i bonds

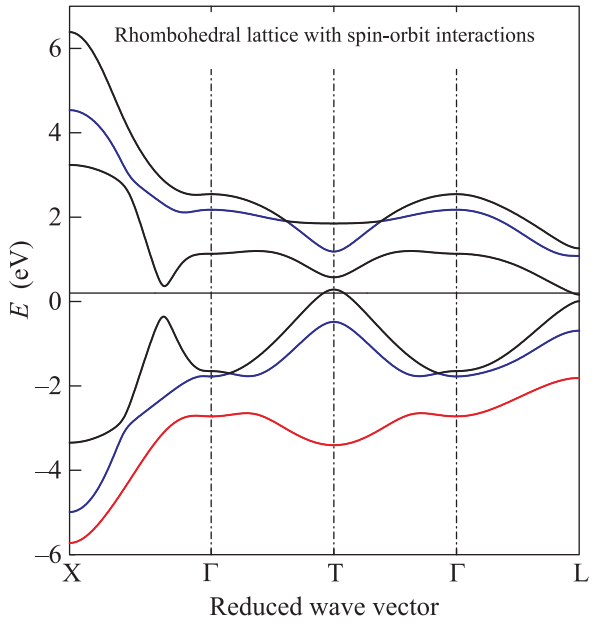

Fig. 4. (Color online) Band structure of a rhombohedral lattice with spin-orbit interactions

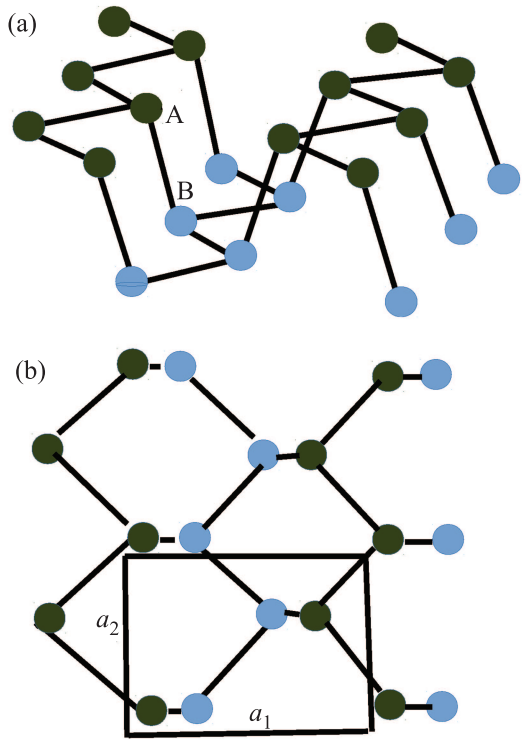

Fig. 5. (Color online) Structure of phosphorene. (a) – 3D representation; the A and B atoms belong to two planes constituting puckered monolayer phosphoren (see text). (b) – Top view; the a_1, a_2 box shows the unit cell with four atoms

hybridized weakly with the deep s bonds. Therefore, we should to work with the low energy Hamiltonian at least as a 12×12 matrix. Thus, we have to determine, first, the symmetric prophase and, second, the doubling and deformational potentials, Eqs. (5), (6).

The situation can be simplified, if we determine correctly the zero-order Hamiltonian. In phosphorene, each atom is connected with the nearest-neighbors by three p_i bonds, $i = x, y, z$. There are two bonds [16] of 2.16 Å and one bond of 2.21 Å, two bond angles are 103.7° and one bond angle is 98.1°. Let three p_i bonds are equal in value and the angles between the bonds are 90°. We obtain two parallel planes with the distance a between the nearest atoms (see Fig. 6). One puckered monolayer of

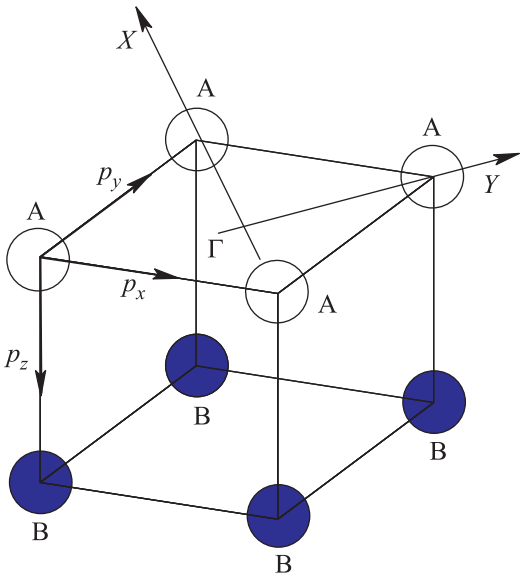

Fig. 6. (Color online) Cubic prophase of phosphorene, the p_i orbitals are shown; the ΓX and ΓY directions are identical to thous in Fig. 7

phosphorene is turned to two parallel planes with two atoms A and B in the unit cell and with the translation symmetry in x and y directions. The Hamiltonian of the zero-order could be obtained, if we combine the 3×3 matrix $\mathcal{A}$, connecting nearest neighbors of the A type, with the matrix $\mathcal{B} = \mathcal{A}$, connecting the neighbors of the B type. The matrix $\mathcal{A}_{\rm B}$, connecting the atoms of the A and B type, appears as well. Thus, we get the Hamiltonian in the form of the 6×6 matrix

$$A(\mathbf{k}) = \begin{pmatrix} \mathcal{A} & \mathcal{A}_{\rm B} \\ \mathcal{A}_{\rm B}^{\dagger} & \mathcal{A} \end{pmatrix}. \qquad (11)$$

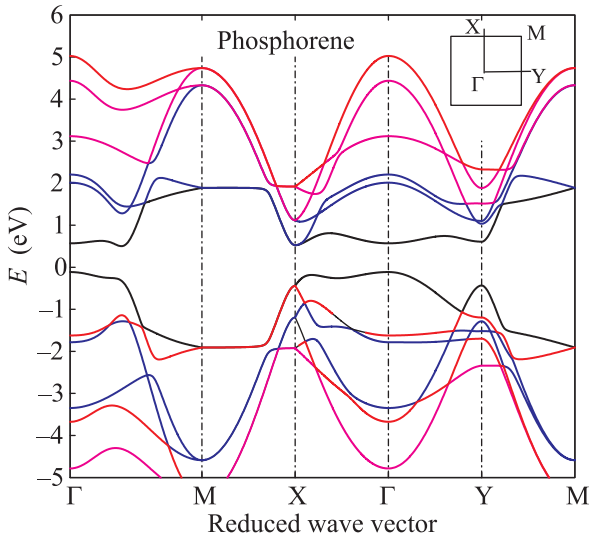

Fig. 7. (Color online) Band structure for the black phosphorus monolayer

The matrix elements of this matrix are obtained as the hopping integrals of the cubic Hamiltonian H_0 between the p_i orbitals centered on two atoms A and B:

$$\begin{gathered}\mathcal{A}_{xx} = \xi_0 \cos k_x a + \xi_1 \cos k_y a + \eta_2 \cos k_x a \cos k_y a,\\ \mathcal{A}_{yy} = \xi_0 \cos k_y a + \xi_1 \cos k_x a + \eta_2 \cos k_y a \cos k_x a,\\ \mathcal{A}_{zz} = \xi_1(\cos k_x a + \cos k_y a) + \eta_1 \cos k_x a \cos k_y a,\\ \mathcal{A}_{xy} = \mathcal{A}_{yx} = \eta_0 \sin k_x a \sin k_y a,\\ \mathcal{A}_{xz} = \mathcal{A}_{zx} = \mathcal{A}_{yz} = \mathcal{A}_{zy} = 0,\\ \mathcal{A}_{\mathrm{B}xx} = 0.5\eta_1 \cos k_y a + \eta_2 \cos k_x a(\cos k_y a + 0.5),\\ \mathcal{A}_{\mathrm{B}yy} = 0.5\eta_1 \cos k_x a + \eta_2 \cos k_y a(\cos k_x a + 0.5),\\ \mathcal{A}_{\mathrm{B}zz} = 0.5\xi_0 + \eta_1 \cos k_x a \cos k_y a + \\ + 0.5\eta_2(\cos k_x a + \cos k_y a),\\ \mathcal{A}_{\mathrm{B}xz} = 0.5i\eta_0 \sin k_x a, \mathcal{A}_{\mathrm{B}yz} = 0.5i\eta_0 \sin k_y a,\\ \mathcal{A}_{\mathrm{B}zx} = -\mathcal{A}_{\mathrm{B}xz},\ \mathcal{A}_{\mathrm{B}zy} = -\mathcal{A}_{\mathrm{B}yz},\ \mathcal{A}_{\mathrm{B}xy} = \mathcal{A}_{\mathrm{B}yx} = 0\end{gathered} \tag{12}$$

with ξ and η having the same meaning as in Eq. (4). Here we take into account that the vector $\mathbf{k}$ has only two components k_x and k_y.

The Hamiltonian of Eq. (6) has the orthorhombic symmetry C_{2h} in the case of phosphorene. The corresponding matrix elements

$$\begin{gathered}E_{xx} = e_1 \cos k_x a + e_2 \cos k_y a,\\ E_{yy} = e_1 \cos k_y a + e_2 \cos k_x a,\\ E_{zz} = e_3(\cos k_x a + \cos k_y a),\\ E_{xy} = e_{12}(\cos k_x a + \cos k_y a),\\ E_{xz} = e_{13} \cos k_x a + e_{23} \cos k_y a,\\ E_{yz} = e_{13} \cos k_y a + e_{23} \cos k_x a\end{gathered} \tag{13}$$

should be added to the matrix $\mathcal{A}$.

Now we have to include the Peierls doubling. If two primitive vectors of the cubic lattice in the x, y plane are denoted as $a(10)$ and $a(01)$, then the lattice with the doubling unit cell has the primitive vectors $\mathbf{a}_1 = a(-1, 1)$ and $\mathbf{a}_2 = a(1, 1)$, these are the X and Y directions in Fig. 6 with Y in the symmetry plane and X along the two-fold axis of phosphorene. The primitive vectors of the reciprocal lattice are

$$\mathbf{Q}_1 = \pi(-1, 1)/a, \quad \mathbf{Q}_2 = \pi(1, 1)/a. \tag{14}$$

Because the vectors $\mathbf{k}$ and $\mathbf{k} + \mathbf{Q}_2$ are equivalent in the Brillouin zone after doubling in the $\mathbf{Q}_2$ direction (this is the Y direction in phosphorene, see Fig. 6), we have to combine the matrices $A(\mathbf{k})$, Eq. (11), and $A(\mathbf{k} + \mathbf{Q}_2)$ into the 12×12 matrix in much the same way as in Eq. (7). The U matrix has the form

$$U(\mathbf{k}) = \begin{pmatrix} \mathcal{UA} & 0 \\ 0 & \mathcal{UA} \end{pmatrix} \tag{15}$$

with the matrix elements of the orthorhombic Hamiltonian, Eq. (5), as following:

$$\begin{gathered}\mathcal{UA}_{xx} = u_1 \sin k_x a + u_2 \sin k_y a,\\ \mathcal{UA}_{yy} = u_1 \sin k_y a + u_2 \sin k_x a,\\ \mathcal{UA}_{zz} = u_3(\sin k_y a + \sin k_x a),\\ \mathcal{UA}_{yx} = \mathcal{UA}_{xy} = 0,\\ \mathcal{UA}_{zx} = \mathcal{UA}_{xz} = 0,\\ \mathcal{UA}_{zy} = \mathcal{UA}_{yz} = 0.\end{gathered} \tag{16}$$

The spin-orbit interaction Δ_{so} is sometimes pointed out as a possible source of contradictions in the calculations of the band structure. Because the spin-orbit interaction is proportional to the ion charge squared and $\Delta_{so} = 1.2\,\mathrm{eV}$ in bismuth, we can estimate the spin-orbit value for BP as $\Delta_{so} \approx 0.04\,\mathrm{eV}$, i.e. much smaller in comparison with the interesting energy of the order of 0.2 eV in BP. Therefore, the spin-orbit coupling cannot noticeably change the quasiparticle band structure in phosphorus [11].

The band structure obtained for phosphorene is shown in Fig. 7 with the following values of the hopping integrals (in eV): $\xi_0 = 3.9$, $\xi_1 = -0.68$, $\eta_0 = -0.3$, $\eta_1 = 0.01$, $\eta_2 = 0.25$, $u_1 = 0.96$, $u_2 = 0.2$, $u_3 = -0.42$, $e_1 = 0.1$, $e_2 = -0.32$, $e_3 = 0.1$, $e_{12} = -0.73$, $e_{13} = -0.23$, $e_{23} = -0.3$. This set gives a semiconductor with the minimal quasiparticle band gap $\varepsilon_g = 0.56\,\mathrm{eV}$ at the Γ point. The band dispersion is more flat along the ΓX direction than in the ΓY direction. Thus we get the effective masses of holes $m_x^{(h)} = 0.35m_0$ and $m_y^{(h)} = 1.04m_0$ corresponding with the values discussed

in Introduction. The effective masses of electrons at Γ have the close values.

IV. Summary. At 4.5 GPa, the phosphore structure changes from the orthorhombic (A-17) symmetry to rhombohedral one (A-7, of bismuth type), which transforms to the sc at 10 GPa. The structure of the orthorhombic and rhombohedral phases differs slightly from the more symmetrical sc structure. Therefore, their quasiparticle dispersion can be obtained using the general Peierls idea of the doubling distortion. We show that in agreement with experiments, the low energy Hamiltonian constructed in accordance with the Peierls method gives the dispersion of a metal for the sc phase, of a semimetal or a narrow gap semiconductor for the A-7 phase, and of a semiconductor for phosphorene. Because of the band gap at different points in the Brillouin zone (Γ, X, and Y) is small, phosphorene can be transformed by compression from direct band gap semiconductor to indirect semiconductor or semimetal.

This research was initiated by V. Brazhkin who called the author's attention to the problem of phosphorene. We acknowledge the Russian Foundation for Basic Research (grant # 13-02-00244A) and the SIMTECH Program, New Centure of Superconductivity: Ideas, Materials and Technologies (grant # 246937).

1. A. H. Castro Neto, F. Guinea, N. M. R. Peres, K. S. Novoselov, and A. K. Geim, Rev. Mod. Phys. **81**, 109 (2009).
2. H. Kawamura, I. Shirotani, and K. Tachikawa, Sol. State Comm. **49**, 879 (1981); **54**, 775 (1985).
3. H. Karuzawa, M. Ishizuka, and S. Endo, J. Phys.: Cond. Mat. **14**, 10759 (2002).
4. K. T. Chan, B. D. Malone, and M. L. Cohan, Phys. Rev. B **88**, 064517 (2013).
5. T. Low, R. Roldán, H. Wang, F. Xia, P. Avouris, L. M. Moreno, and F. Guinea, Phys. Rev. Lett. **113**, 106802 (2014).
6. H. Liu, A. T. Neal, Z. Zhu, D. Tománek, and P. D. Ye, arXiv: 1401.4133.
7. L. Li, Y. Yu, G. J. Ye, Q. Ge, X. Ou, H. Wu, D. Feng, X. H. Chen, and Y. Zhang, arXiv: 1401.4117.
8. M. Buscema, D. J. Groenendijk, S. I. Blanter, G. A. Steele, H. S. J. van der Zant, and A. Castellanos-Gomez, arXiv: 1403.0565.
9. F. Xia, H. Wang, and Y. Jia, arXiv: 1402.0270.
10. Y. Du, C. Ouyang, S. Shi, and M. Lei, J. Appl. Phys. **107,** 093718 (2010).
11. J. Qiao, X. Kong, Z-X. Hu, F. Yang, and W. Ji, arXiv:1401.5045.
12. K. Gong, L. Zhang, W. Ji, and H. Guo, arXiv:1404.7207.
13. Y. Takao and A. Morita, Physica B **105,** 93 (1981).
14. H. Asahina and A. Morita, J. Phys. C: Sol. State Phys. **17**, 1839 (1984); A. Morita, Appl. Phys. A **39,** 227 (1986).
15. A. N. Rudenko and M. I. Katsnelson, Phys. Rev. B **89**, 201408(R)(2014).
16. A. Castelanos-Gomes, L. Vicarelli, E. Prada, J. O. Island, K. L. Narasimha-Acharya, S. I. Blanter, D. J. Groenendijk, M. Buscema, G. A. Steele, J. V. Alvarez, H. W. Zandbergen, J. J. Palacios, and H. S. J. van der Zant, 2D Mater **1**, 025001 (2014).
17. N. B. Goodman, L. Ley, and D. W. Bulett, Phys. Rev. B **27**, 7440 (1983).
18. V. Tran, R. Soklaski, Y. Liang, and L. Yang, Phys. Rev. B **89**, 25319 (2014).
19. A. S. Rodin, A. Carvalho, and A. H. Castro Neto, Phys. Rev. Lett. **112**, 176801 (2014).
20. A. A. Abrikosov and L. A. Falkovsky, ZhETF **43,** 1089 (1962) [Sov. Phys. JETP **16**, 769 (1963)].
21. V. A. Volkov and O. A. Pankratov, ZhETF **75**, 1362 (1978) [Sov. Phys. JETP **48**, 687 (1978)].
22. V. A. Volkov and L. A. Falkovsky, ZhETF **85**, 2135 (1983) [Sov. Phys. JETP **56**, 1239 (1983)].
23. A. E. Dorofeev and L. A. Falkovsky, ZhETF **87**, 2202 (1984) [Sov. Phys. JETP **60**, 1273 (1984)].